FRINGE FIELD INTERFERENCE AND COMPENSATION OF QUADRUPOLES IN THE CSNS RCS

Y. Li*[1,2], Y.W. An[1,2], C.D. Deng[1,2], J.L. Chen[1,2], Z.P. Li[1,2]
[1]Institute of High Energy Physics, Chinese Academy of Sciences, Beijing, China
[2]Spallation Neutron Source Science Center, Dongguan, China

Abstract

During the beam power upgrade of the Rapid Cycling Synchrotron (RCS) at the China Spallation Neutron Source (CSNS), 16 newly installed trim quadrupoles (QT) cause fringe field interference with adjacent main quadrupoles, distorting lattice parameters and increasing beam loss. Using OPERA, MAD-X, and PyORBIT, it is found that QT reduces QD's integrated field by 0.77%, leading to significant tune shifts and over 10% beta-beat, with beam transmission dropping from 99.76% to 82.74% at the operation tunes. Orbit response matrix measurement confirms a 0.7% field reduction, matching simulations. A compensation scheme successfully reduces beam loss, supporting the beam power upgrade.

INTRODUCTION

As the performance requirements of modern accelerators continue to increase, magnet layouts are becoming increasingly compact. Constrained by physical design considerations and tunnel space limitations, the distance between adjacent magnets is continuously reduced, causing the iron cores of magnets to inevitably extend into each other's fringe field regions. This alteration of fringe field distribution due to the presence of adjacent iron cores, along with its corresponding impact on beam dynamics, is referred to as the fringe field interference effect. This effect induces variations in the integrated magnetic field [1], subsequently leading to issues such as tune shifts and optical parameter distortion. In high-intensity accelerators, it may even cause catastrophic beam loss, severely limiting performance enhancement.

Multiple laboratories worldwide have conducted systematic research on fringe field interference effects. For instance, the Beijing Electron-Positron Collider II (BEPC-II) pioneered the use of 3D multipole expansion techniques to investigate such fringe field interference effects in quadrupole-sextupole combined magnets, achieving an excellent agreement between simulations and experimental results [2]. At the Spallation Neutron Source (SNS) storage ring in the United States, closely packed large-aperture quadrupole magnets in the straight sections were found to exhibit an integrated gradient reduction of more than 1% due to fringe field interference [3]. For the CSNS RCS, the compact layout between large-aperture quadrupoles and adjacent sextupoles has been shown to cause a 2.3% reduction in the integrated gradient of the quadrupoles, leading to significant tune shifts and optical distortions [4]. However, the interference effect between the newly added trim quadrupole magnets (QT), installed for subsequent beam power upgrades, and the main quadrupole magnets has not yet been systematically evaluated. Building upon previous work [4], this paper focuses on investigating the interference effect between the additionally installed trim quadrupoles and the adjacent main quadrupoles in CSNS RCS.

* liyong@ihep.ac.cn

CSNS OVERVIEW

The CSNS RCS [5] has a circumference of 227.92 m and adopts a four-fold symmetric lattice based on triplet focusing structures. A total of 48 main quadrupole magnets are installed in the RCS, which are divided into five families with each powered by a common resonant power supply. To address challenges including optical parameter correction and space charge compensation for high-intensity beams, 24 positions for trim quadrupole magnets were reserved in the initial design of the CSNS RCS [6]. Operational experience has shown that when the beam power exceeds 100 kW, relying solely on the main quadrupoles is insufficient to meet the requirements for optical parameter adjustment [7]. Consequently, 16 programmable trim quadrupoles were additionally installed in the RCS.

Figure 1 shows the actual installation layout of a QT magnet in the accelerator tunnel. As shown, the QT is installed at one end of a main quadrupole (QD), with both magnets sharing a ceramic vacuum chamber with an inner diameter of 272 mm. Constrained by the tunnel installation space, the maximum allowable longitudinal installation length is only 200 mm. Through optimized design, the final iron core length of the QT magnet was determined to be 150 mm. In this extremely compact configuration, the magnetic fields of the QD and QT inevitably extend into each other's fringe field regions, resulting in a significant fringe field interference effect.

3D ELECTROMAGNETIC SIMULATION

To quantitatively evaluate the fringe field interference effect between the QT and QD magnets, a high-precision magnetic field model was first established via the 3D electromagnetic field simulation software OPERA/TOSCA for the systematic analysis of their mutual magnetic influence. Figure 2 shows the 3D simulation model constructed in OPERA/TOSCA, which strictly follows the actual dimensions and end-chamfering angles of the QD and QT magnets. For the accurate simulation of magnetic field distribution, mesh refinement was implemented in the magnet gap and fringe field regions, with a minimum mesh size of 2 mm to

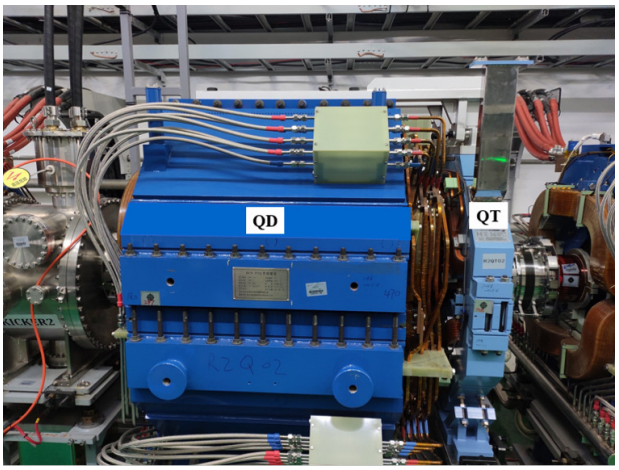

Figure 1: The main quadrupole (QD) with a trim quadrupole (QT) in the tunnel.

ensure analytical accuracy in these regions. The boundary conditions were set as parallel magnetic flux boundaries, with a calculation region of 1.5 m × 1.5 m × 2.0 m, ensuring that the fringe field decays to a negligible level.

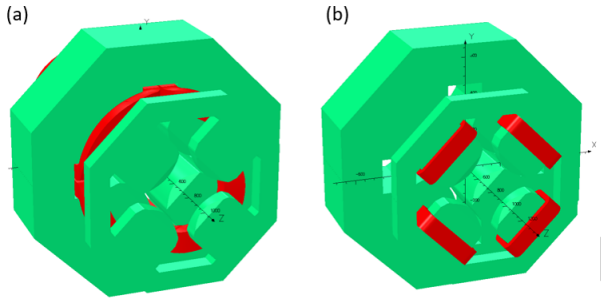

Figure 2: 3D simulation model for fringe field interference.

First, the fringe field interference effect of the QT on the QD was simulated and analyzed (Fig. 2(a)). In this simulation, the QD was excited at its maximum DC design current, while the QT was off. The simulation results show that, compared to the ideal state without the QT, the presence of the QT causes a 0.77% reduction in the integrated field strength of the QD. Second, the reverse interference effect was simulated (Fig. 2(b)), i.e., the QD was off while the QT was excited at its maximum DC design current. Compared to an ideal reference model without the QD, the simulation results indicate that the presence of the QD iron core increases the integrated field strength of the QT by 1.9%.

IMPACT ON BEAM DYNAMICS

To systematically evaluate the impact of the interference effect between the QT and QD magnets on lattice parameters and beam dynamics, theoretical calculations of the global tune and beta-function distortion were first performed using the MAD-X program. Since the QT is a trim quadrupole magnet, small variations in its integrated field exert a relatively minor perturbation on the overall lattice; therefore, the study focuses primarily on the effect induced by the 0.77% decrease in the integrated field of the main quadrupole QD.

Table 1 shows the tune shifts resulting from the fringe field interference. The results indicate that a 0.77% decrease in the QD's integrated field induces significant shifts in both typical operating points: for the design operating point (4.86, 4.80), the horizontal tune increases to 4.89, while the vertical tune decreases to 4.68; for the alternative operating point (4.80, 4.86), the horizontal tune increases to 4.828, while the vertical tune decreases to 4.746. It is particularly noteworthy that the vertical tune of the design operating point drops from 4.80 to 4.68, bringing it closer to the half-integer resonance line (Q_y = 4.5). It can be predicted that without tune correction, the combined effects of space charge and the half-integer resonance would severely degrade the quality of high-power beams.

Table 1: Impact Of Fringe Field Interference On The Tunes

Betatron Tune	(Q_x, Q_y)
Original Tunes	(4.86, 4.80) & (4.80, 4.86)
Tunes with interference	(4.89, 4.68) & (4.828, 4.746)

Figure 3 shows the beta-function distortion (beta-beat) caused by the fringe field interference. The simulation results indicate that the horizontal beta-function variation is negligible, while the vertical beta-function distortion exceeds 10%. Based on previous operational experience, a beta-beat of this magnitude induces additional beam loss during beam injection and acceleration, which necessitates compensation via optical parameter correction.

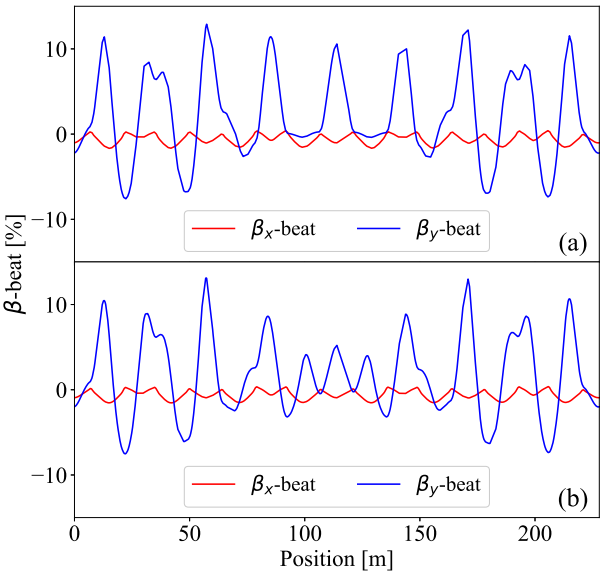

Figure 3: Beta-beat caused by fringe field interference.

To further evaluate the impact of the fringe field interference on high-power beams, numerical simulations were conducted using the multi-particle tracking code PyORBIT [8], which is based on the Particle-in-Cell (PIC) algorithm. This code can simulate space charge effects and the beam injection process, and has successfully reproduced several experimental results of the CSNS RCS, such as beam loss

and bunching factor [9]. In the simulations, the actual lattice structure and aperture constraints were adopted.

Figure 4 shows a comparison of the particle survival rates in the ring with and without fringe field interference. Figure 4(a) and 4(b) correspond to the design operating point and the actual operating point (injection: (4.80, 4.86), extraction: (4.77, 4.77)). The simulation results demonstrate that fringe field interference leads to a significant increase in beam loss. At the design operating point, this interference effect causes particle losses exceeding 50% within 200 turns. At the actual operating point, the beam transmission rate drops sharply from 99.76% to 82.74%.

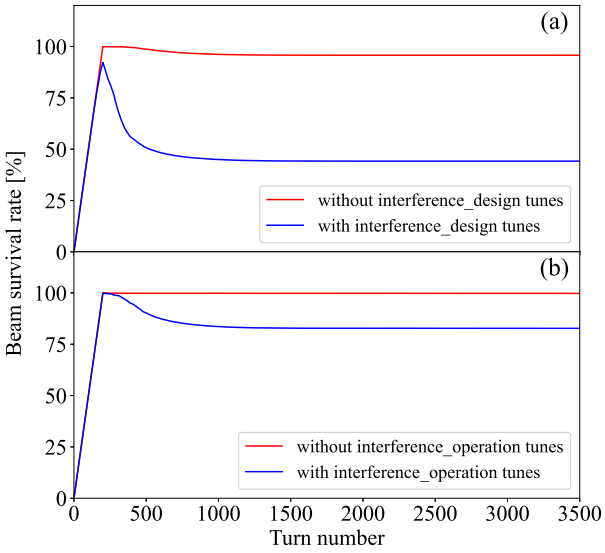

Figure 4: Simulation results of particle loss caused by fringe field interference.

MEASUREMENT AND COMPENSATION

To quantitatively evaluate the fringe field interference effect between the QT and QD magnets, an accelerator optics diagnostic method based on the orbit response matrix was employed in this study.

The experiment was conducted in DC mode (80 MeV) with the operating point set to (4.86, 4.80). To avoid beam loss caused by orbit variations under high power operation, the beam power was controlled below 10 kW. To ensure that the response matrix reflected only the focusing characteristics of the QD magnets, the QT power supplies were turned off during the measurement process.

After completing the orbit response matrix measurement, the obtained data were analyzed using the LOCO (Linear Optics from Closed Orbits) program [10] developed at SLAC. The analysis results show that the fudge factor for the QD magnets is 0.993 (i.e., the ratio of actual to theoretical field strength), indicating that the actual magnetic field strength is approximately 0.7% lower than the theoretical design value. This measurement result is in excellent agreement with the 0.77% reduction predicted by the earlier OPERA 3D electromagnetic field simulations, which strongly validates the reliability of the simulation model.

Based on these experimental results, a current compensation scheme for the QD magnets was implemented in subsequent beam commissioning, i.e., the actual operating current was adjusted to 1.007 (1/0.993) times the theoretical value to restore their equivalent focusing strength. To verify the effectiveness of the compensation scheme, comparative experiments were conducted at a beam power of 100 kW, with the operating point set to the actual operational mode. Figure 5 shows the variations in beam loss within the ring before and after compensation. The results demonstrate that beam loss was significantly reduced after the implementation of the compensation scheme. It is particularly noteworthy that the beam loss trend observed experimentally (Fig. 5) is in excellent agreement with the PyORBIT simulation results (Fig. 4 (b)), which confirms the effectiveness of the compensation scheme and further validates the accuracy of the multi-particle tracking simulation program.

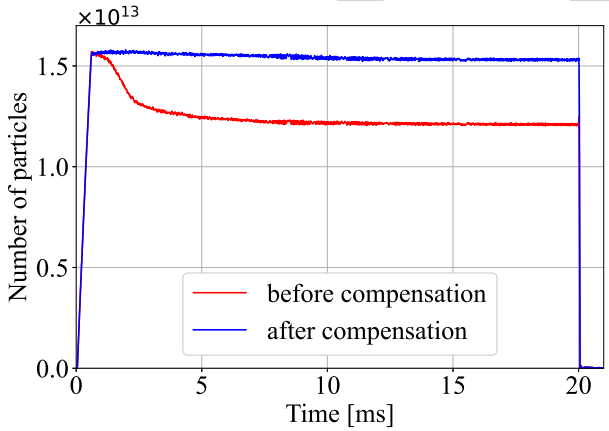

Figure 5: Comparison results of beam loss before and after fringe field interference compensation.

CONCLUSION

This study comprehensively reveals the fringe field interference effect between the newly added trim quadrupoles and main quadrupoles in the compact magnet layout of the CSNS RCS. The current compensation scheme has been successfully applied in actual beam commissioning of the CSNS RCS, which effectively reduces beam loss in high-power operation. These results not only provide critical technical support for the 500 kW beam power upgrade of the CSNS, but also provide important design references for the compact magnet layout of other high-intensity proton accelerators.

REFERENCES

[1] M. J. Shirakata, H. Fujimori, and Y. Irie, "Upgraded Symplectic 3D Beam Tracking of the J-PARC 3 GeV RCS", in *Proc. EPAC'04*, Lucerne, Switzerland, paper THPLT071, pp. 2658–2660, Sep. 2004. http://accelconf.web.cern.ch/e04/papers/THPLT071.pdf

[2] Y. Chen, S. Wang, Q. Qin, W. Kang, Q. Peng, and S. Fang, "Fringe field interference research on quadrupole-sextupole assembly in bepc-ii", *IEEE Trans. Appl. Supercond.*, vol. 24, no. 3, pp. 1–4, 2013. doi:10.1109/TASC.2013.2282662

[3] JG. Wang, N. Tsoupas, and M. Venturini, "3d-simulation studies of sns ring doublet magnets", in *Proc. PAC'05*, pp. 3865–3867, 2005. doi:10.1109/PAC.2005.1591650

[4] J. Chen, S. Xu, X. Lu, Y. An, Y. Li, and S. Wang, "Study on the fringe field and the field interference effects of quadrupoles in the rapid cycling synchrotron of the china spallation neutron source", *Nucl. Instrum. Methods Phys. Res. A*, vol. 927, pp. 424–428, 2019. doi:10.1016/j.nima.2019.03.002

[5] W. Sheng *et al.*, "Introduction to the overall physics design of csns accelerators", *Chinese Physics C*, vol. 33, no. S2, pp. 1–3, 2009. doi:10.1088/1674-1137/33/S2/001

[6] Y. An and S. Wang, "The compensation of quadrupole errors and space charge effects by using trim quadrupoles", *Sci. China Phys., Mech. Astron.*, vol. 54, no. Suppl 2, pp. 214–217, 2011. doi:10.1007/s11433-011-4566-8

[7] Y. Li *et al.*, "Applications of programmable trim quadrupoles on beam commissioning for the csns rcs", *J. Instrum.*, vol. 19, no. 03, T03003, 2024. doi:10.1088/1748-0221/19/03/T03003

[8] A. Shishlo, S. Cousineau, J. Holmes, and T. Gorlov, "The particle accelerator simulation code pyorbit", *Procedia Comput. Sci.*, vol. 51, pp. 1272–1281, 2015. doi:10.1016/j.procs.2015.05.312

[9] L. Huang *et al.*, "Longitudinal dynamics study and optimization in the beam commissioning of the rapid cycling synchrotron in the china spallation neutron source", *Nucl. Instrum. Methods Phys. Res. A*, vol. 998, p. 165204, 2021. doi:10.1016/j.nima.2021.165204

[10] J. Safranek, G. Portmann, and A. Terebilo, "MATLAB-BASED LOCO", in *Proc. EPAC'02*, Paris, France, paper WEPLE003, pp. 1184–1186, Aug. 2007. https://jacow.org/e02/papers/WEPLE003.pdf